Analysis of angle-resolved photoemission data of PbS (001) surfaces within the direct-transition model

R. Böttner, S. Ratz, N. Schroeder, S. Marquardt, and U. Gerhardt
Physikalisches Institut der Universität, Robert Mayer-Straβe 2-4, D-60054 Frankfurt, Germany

R. Gaska
Department of Electrical and Computer Engineering, Wayne State University, Detroit, Michigan 48202

J. Vaitkus
Semiconductor Physics Department, Vilnius University, Sauletekio al. 9-III, 2054 Vilnius, Lithuania
(Received 2 October 1995)

We measure angle-resolved photoelectron spectra of PbS (001) surfaces excited by synchrotron radiation. A great deal of experimental data including normal and off-normal emission for a variety of photon energies and emission angles are discussed. We also compare series of spectra recorded with the polarization vector parallel and perpendicular to the (100) observation plane. It is shown that most of the angle-resolved photoemission spectroscopy structures can be explained readily within the three-step model of photoemission invoking direct transitions, and that the experimental results agree very well with pseudopotential band-structure calculation. In order to investigate the influence of spin-orbit coupling (SOC) on both the eigenvalues and selection rules we compare our data with two theoretical calculations, one including SOC, the other neglecting it.

I. INTRODUCTION

The investigation of complex materials such as high-temperature superconductors or heavy-fermion systems by means of angle-resolved photoelectron spectroscopy (ARPES) requires special reliability concerning the interpretation of the experimental data. Therefore, a detailed knowledge of the underlying excitation process is required, and the applicability of certain approximations used for the analysis of the spectra has to be marked out.

Most people active in the field of photoemission analyze their data in terms of the conventional three-step model.[1] Within this simple picture ARPES structures are caused by direct transitions between bands in the reduced zone scheme of the reciprocal space. Despite the large number of materials discussed successfully within this model, doubts were issued frequently about its universal applicability. Critics claimed that the finite lifetime of the excited photoelectron should effectively relax the momentum conservation of the component $k_\perp$ perpendicular to the crystal surface. Carried to the extreme, this idea would yield a complete ''smearing'' of $k_\perp$ over the dimension of the Brillouin zone as it is assumed in the ''one-dimensional density of states'' (ODDS) model. Within this picture all transitions along the line $k_\parallel =$ const of the Brillouin zone contribute to a photoemission spectrum, which should, consequently, reflect singularities in the density of initial states along this line.

Some authors analyzed their data completely within this model,[2] others relied on a modified version called ''weighted indirect transition model.''[3] Grandke, Ley, and Cardona,[3] used both models to deal with ARPES measurements performed on the lead chalcogenides and claimed a good agreement of the experimental data with predictions of the ODDS model, at least for off-normal emission. Considering the results presented in this paper, we feel that it is quite inappropriate to use the ODDS model as a starting point for the description of the photoemission process: owing to the vanishing momentum of ultraviolet photons the optical excitation is in principle a direct transition. Damping effects can be treated by adding an imaginary part to the periodic potential. This leads to the finite linewidths of the ARPES structures and may cause small shifts in the energy of the transition. However, this effect should not be treated in a manner that assigns the predominant importance to a minor perturbation as it is done in the ODDS model.

Moreover, the ODDS model must fail by its definition when one tries to explain any dispersion of ARPES peaks along the lines of k space perpendicular to the sample surface, e.g., normal emission. Therefore, if the off-normal data could be explained by direct transitions as well, there seems to be no need at all to use a model that neglects the conservation of the wave vector.

For that reason we thought it worthwhile to reinvestigate a member of the lead chalcogenides, namely, PbS, and try to analyze the results completely within the conventional direct transition model. The basics of this model are outlined below. The analysis is performed using the final states obtained by a slightly modified pseudopotential calculation published by Kohn *et al.*,[4] which also will be discussed below. Section IV gives a short review of the experimental setup and in Sec. V we describe the procedure of comparing experiment and theory. Finally, the experimental results are presented and discussed (Sec. VI).

II. PHOTOEMISSION

As mentioned above we analyze all our experimental data utilizing the conventional three-step model of photoemission.[1] In this picture energy and momentum conservation have to be fulfilled both for optical excitation (first step)

and for electron escape into vacuum (third step). Because momentum transfer of ultraviolet photons is negligible, the first step is characterized by the expressions

$$E_f - E_i = \hbar\omega, \quad \mathbf{k}_f = \mathbf{k}_i(+\mathbf{G}) = \mathbf{k}.$$

According to Fermi's ''golden rule'' the transition probability in the dipole approximation is proportional to the square of the transition matrix element

$$w_{if} \sim |\langle f|\mathbf{e}\cdot\mathbf{p}|i\rangle|^2,$$

where **e** indicates the polarization vector of the incident radiation. This expression leads to a parity selection rule first formulated by Hermanson,[5] which holds for emission in a mirror plane of the crystal if spin-orbit coupling (SOC) is negligible. According to this rule the initial state must have positive parity for parallel polarization and negative parity for perpendicular polarization. Since SOC mixes states with different spatial symmetries,[6] this rule appears to be more or less relaxed in systems with heavy atoms like PbS.

The third step of photoemission requires

$$E_f - E_{\rm vac} = E_{\rm kin}, \quad k_{\parallel,\rm vac} = k_\parallel(+G_\parallel).$$

Because the potential barrier at the surface changes only $k_\perp$, momentum conservation holds still for $k_\parallel$. In the following we focus our discussion to the much more pronounced primary cone emission with no surface umklapp, i.e., $G_\parallel = 0$. The parallel component of the wave vector can be calculated immediately using the well-known expression

$$k_\parallel = [(2mE_{\rm kin})^{1/2}/\hbar]\,\sin\theta,$$

where θ indicates the emission angle measured with respect to the surface normal.

III. BAND-STRUCTURE CALCULATION

The simplest and most often employed method to determine the unknown component $k_\perp$ of the wave vector is based on the assumption of a free-electron final state $E_f = \hbar^2k^2/2m^* + V_0$ with adjustable parameters for the effective mass m^* and the inner potential V_0. As demonstrated by Hinkel *et al.*,[7] this rough approximation seems to be working moderately in the case of the normal emission data in PbSe and PbTe. However, it seems uncertain if it is also valid for off-normal emission. In fact, for PbS we could not obtain convincing results for both normal and off-normal emission. For that reason we decided to use a more accurate approximation of the final states utilizing a pseudopotential band-structure calculation, employing the slightly modified Fourier coefficients, already published by Kohn *et al.*[4] For reasons of convergence we had to include reciprocal lattice vectors up to $|G_{\rm max}|^2 = 20$ (in units of $2\pi/a$). This corresponds to $N = 113$ plane waves for each spin orientation, which is probably a larger number than that used by Kohn *et al.* Unfortunately, in this approximation we could not reproduce the well-known value of the direct energy gap at the L point.

However, this shortcoming could be corrected by altering the coefficient $V_s(4)$ (-0.2532 Ry in the work of Kohn *et al.*) to -0.2689 Ry, resulting in a magnitude of 0.4 eV for the gap, which closely resembles the experimental value at room temperature. Table I summarizes the numerical quantities of both the pseudopotential coefficients and the spin-orbit parameters used in the calculation.

TABLE I. Numerical values of the pseudopotential form factors and spin-orbit coupling parameters.

Pseudopotential form factor (Ry)					SOC parameter	
$V_A(3)$	$V_S(4)$	$V_S(8)$	$V_A(11)$	$V_S(12)$	λ_S	λ_A
0.0859	-0.2689	-0.0181	0.010 38	0.0242	0.103	0.093 42

In order to investigate the influence of SOC on both the eigenvalues and the selection rules we calculated two band structures, with and without SOC taken into account. We compare most of our data with both calculations.

IV. EXPERIMENT

The experimental setup used in our work is described in full detail in Ref. 8. We thus restrict ourselves to the description of the main features. All measurements were performed at the 2m Seya beamline of the Berliner Elektronenspeicherring für Synchrotronstrahlung (BESSY). The electron analyzer we used is capable of detecting eight emission angles in the plane of observation simultaneously. A variation of these directions can be achieved by rotating the sample relative to the analyzer. In the standard configuration the polarization vector **e** of the radiation lies within the plane of observation. Spectra with perpendicular polarization can be also recorded by rotating the analyzer about the axis of the incoming beam. The angular resolution of the electron monochromator is 2° full width at half maximum, the total energy resolution of both the 2m Seya and the analyzer was set to approximately 100–150 meV for most of the measurements.

High-quality crystals of PbS were grown by a slow cooling method described in Ref. 9. In order to produce clean surfaces we cleaved the samples in the ultrahigh vacuum chamber ($p \approx 2\times10^{-10}$ mbar) either by guiding a razor blade to the edge of the crystals or by peeling off thin copper tabs that were attached to the samples by a suitable glue before installation. Quality and crystallographic orientation of the surfaces were frequently checked by low-energy electron diffraction. Most of the samples turned out to be highly stable in vacuum. No signs of contamination or other modifications could be detected after periods up to 80 h.

V. DATA ANALYSIS

In most cases we recorded ARPES spectra in a binding energy range of approximately 6 eV below the valence-band maximum. The experimental spectra usually exhibit several peaks. They contribute to the total spectrum with varying intensities and widths, depending on the particular measuring geometry and photon energy. In order to determine the energy position of each structure with an accuracy as high as possible, we fitted the spectra with a linear combination of Lorentzians and used the results of this line-shape analysis for further evaluation.

Energy conservation in the emission process requires

$$E_f^{\text{expt}} - E_{\text{vac}} = E_{\text{kin}}.$$

Hence, E_f^{expt} can be determined immediately. Since we know the component $k_\parallel$ of the wave vector, this equation defines a set of values $\{k_\perp^{(j)}\}$ where the calculated bands cross the final-state energy E_f^{expt} along the line $k_\parallel$=const. Which of these are right, or at least most likely, can be determined using the energy conservation at the optical excitation, i.e.,

$$E_i^{\text{expt}} = E_f^{\text{expt}} - \hbar\omega$$

and choosing the one with the smallest deviation between experimental and theoretical values:

$$\left| E_i^{\text{th}}(k_\parallel, k_\perp^{(j)}) - E_i^{\text{expt}} \right| \underset{j}{\rightarrow} \text{min}.$$

Both initial and final states of the photoexcitation are determined by selecting the suitable $k_\perp$. For the bands calculated without SOC one could check if the particular transition is allowed according to the Hermanson rule.

VI. RESULTS AND DISCUSSION

A. Normal emission

We first discuss the most common approach for band-structure determination. The experimental spectra of a normal emission series along the ΓX line in the Brillouin zone are shown as dots in Fig. 1, whereas the results of the fitting procedure are depicted as solid lines approximating these points. The three spectra in the inset were recorded for a smaller energy range in order to verify the very existence of a weak structure and follow its dispersion. These weak structures are also observable in the three lowest spectra (15,16, and 16.5 eV) of the main series. It should be noted that the structure with the smallest binding energy is in fact com-

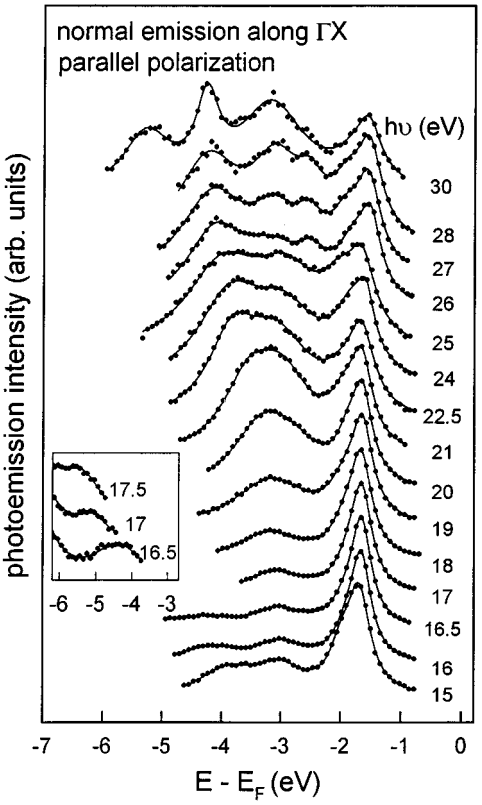

FIG. 1. ARPES spectra of PbS (dots), recorded in normal emission for $\hbar\omega$ between 15 and 30 eV. The solid lines are the result of a least-squares fit. Both the experimental data and the fit lines are shown in the fit region only.

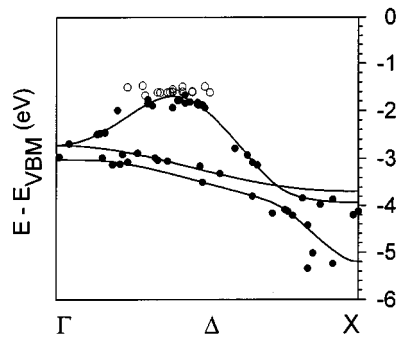

FIG. 2. Calculated bands of PbS (including SOC) along the symmetry line Δ and the measured initial-state energies (filled circles) as determined from the spectra of Fig. 1. The open circles are derived from a dispersionless structure as discussed in the text.

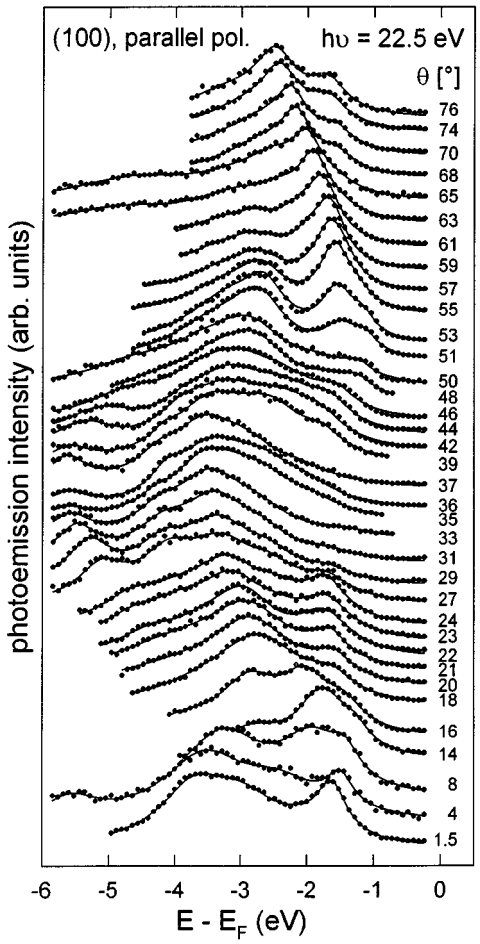

FIG. 3. ARPES spectra of PbS, recorded for $\hbar\omega$=22.5 eV and parallel polarization with respect to the (100) observation plane. The emission angle θ varies between 1.5° and 76°. Both spectra (dots) and fit curves (lines) are shown only in the fit region.

posed of two single lines with energies very close to each other. One of these peaks remains stationary when changing the photon energy. As will be discussed below this may be an indication of a surface state.

In Fig. 2 the results of the data analysis explained in the preceding paragraph are superimposed to the three p-type valence bands along the symmetry line Δ. The points derived from the almost stationary peak at approximately -1.5 eV are depicted as open circles, since they may not be characteristic for the volume bands.

One can see that for some minor discrepancies that occur mainly due to the presence of the weak structure shown in the inset of Fig. 1, experimental results coincide very well with theoretical band calculations.

B. Off-normal emission at fixed photon energies

A number of experiments for various angles of emission and with constant $\hbar\omega$ were carried out. Series of that kind were taken for $\hbar\omega = 22.5$, 21, 19.5, and 15.7 eV, all of them recorded with the polarization vector parallel to the (100) detection plane. As an example, we show in Fig. 3 the spectra for the case of $\hbar\omega = 22.5$ eV. The results of the data analysis are demonstrated in the three panels on the left-hand side of Figs. 4(a)–4(c). The uppermost panel (a) contains the experimental results alone, while (b) and (c) also include theoretical values. As expected, the overall agreement is best for the lowest panel (c). Apart from this quantitative effect, the calculation without SOC suffers from another shortcoming. This is due to the prediction of the Hermanson rule, which classifies all transitions starting from the initial states with odd parity as forbidden in the case of parallel polarization. Such points are depicted as open triangles in Fig. 4. Note that in particular the highly dispersive branch around -5 eV consists mainly of such ''forbidden'' transitions, although the corresponding structures are clearly detectable in the ARPES data. This demonstrates the ''softening'' of selection rules due to the strong SOC in lead sulphide.

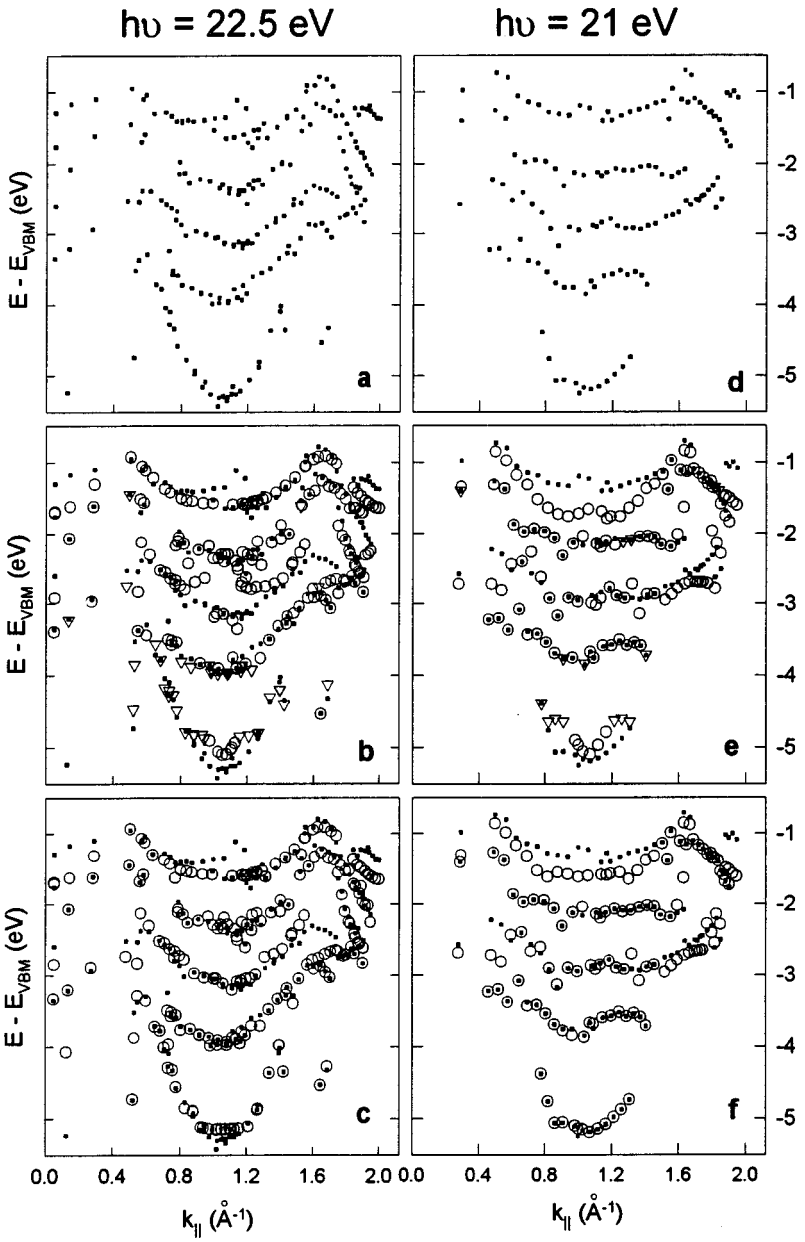

FIG. 4. (a) Experimental initial-state energy as a function of $k_\parallel$ for the spectra of Fig. 3. (b) Same as (a) but in addition the calculated eigenvalues (without SOC) are shown as open circles (allowed transitions) and triangles (forbidden transitions). (c) Same as (b) but the open circles were derived from the full calculation including SOC. The panels (d)–(f) are constructed in the same fashion as (a)–(c), but correspond to $\hbar\omega = 21$ eV.

A similar analysis was performed for the series with $\hbar\omega=21$, 19.5, and 15.7 eV. The results are summarized in Fig. 4 (right-hand side) and Fig. 5. For each photon energy a three-part diagram is constructed in the same fashion as for $\hbar\omega=22.5$ eV. The general conclusion of this analysis is the same as that for $\hbar\omega=22.5$ eV, i.e., we get a reasonably good agreement between experiment and theory even for the calculation without SOC. However, a number of structures in the spectra would arise due to forbidden transitions if SOC could be neglected (open triangles). This inconsistency is removed and additional quantitative improvement is achieved when dealing with the complete calculation including SOC.

Considering all of the data the most conspicuous deviations between experiment and theory are observed for the structure closed to the valence-band maximum. Particularly clear discrepancies are obtained for small values of $k_{\|}$ (<0.4 Å^{-1}). In this region no theoretical explanation exists for the experimentally determined branch at ≈ -1 eV. For $k_{\|}=0$ the corresponding structure is the same as that already discussed above, i.e., a peak that shows no dispersion in normal emission. The lack of a theoretical counterpart for the off-normal emission agrees well with the suggestion of a surface state mentioned above. However, a final proof of this conjecture is yet missing. Future adsorption experiments might be helpful in clarifying that question.

C. Polarization-dependent measurements

Finally we discuss two series of measurements for variable photon energies at a constant emission angle ($\theta=67.5°$). The data were recorded with the polarization vector both parallel to the observation plane and perpendicular to it. If SOC could be neglected completely, one would expect totally different spectra for both cases: according to the Hermanson rule only states with even parity could con-

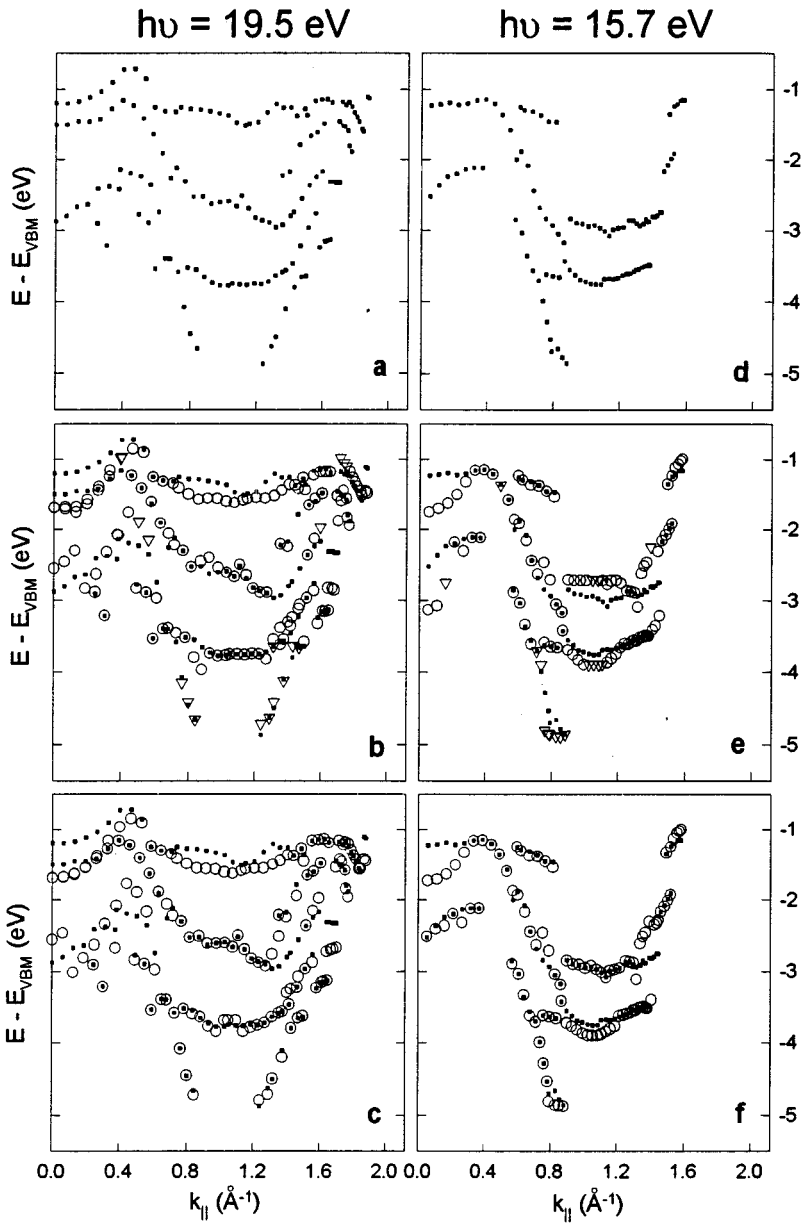

FIG. 5. Same as Fig. 4, but for two other photon energies.

tribute for parallel polarization, and only those with odd parity for perpendicular polarization. Since merely one of the five valence bands has odd parity with respect to the (100) plane, the spectra with parallel polarization should display a higher complexity.

Even if a softening of the selection rules due to SOC is expected to occur, these predictions are qualitatively correct as can be verified by referring to the spectra displayed in Fig. 6. The ARPES data, as well as their fit lines, are drawn solely in the fit region, which was chosen in a way so as to include mainly the dominant features of the spectra. The analysis of peak positions with respect to $k_{\parallel}$ can be seen in Fig. 7.

In spite of the already familiar scheme of this figure, there is a difference in comparison with the analysis we used so far: in order to emphasize the influence of polarization, only the bands with the ''right'' parity were used for comparison in the case without SOC (middle panels). Hence the distinction between allowed and forbidden transitions is useless in this case.

It is obvious from both Fig. 6 and 7 that different states were detected for different polarizations of light. Particularly clear is the case of perpendicular polarization, where merely two structures were found experimentally. Except for $\hbar\omega = 18$ eV and 24 eV$\leqslant\hbar\omega\leqslant$ 28 eV, the peak closer to E_F is much weaker than the other. Both structures move nearly parallel as a function of photon energy. Without SOC, theory can merely account for the lower branch (with generally higher intensity) whereas both branches can be explained by the complete calculation. Again, this is caused by the fact that SOC allows transitions from bands that would have the ''wrong'' parity without SOC.

It is instructive to look closer at the intensity variations visible in the right-hand panel of Fig. 6. They can be understood if we keep track of the locations in the Brillouin zone where the particular transitions take place. For photon energies between 15 and 29 eV the $k_{\parallel}$ components of both peaks vary between approximately 1.2 and 2.25 Å^{-1}. Since the ''distance'' ΓX is ≈ 1.06 Å^{-1}, this corresponds to locations in one of the higher Brillouin zones of the repeated zone scheme. By reducing the values of $k_{\parallel}$ to the first zone, the direction of motion is reversed; i.e., an increase of photon energy leads to a decrease of $|k_{\parallel}^{\text{red}}|$. Between $\hbar\omega\approx 20$ and 27 eV the values of $k_{\perp}^{\text{red}}$ are close to zero, which corresponds to a path in the immediate vicinity of the symmetry line Δ. Noticeable deviations of the path from Δ take place only for $\hbar\omega<20$ eV and $\hbar\omega>27$ eV. Within this range one can compare the dispersion of peaks visible in Fig. 7(d) approximately with the bands along Δ (see Fig. 2). Note, however, the reversed direction of motion ($X\Gamma$).

The flat part of the bands in Fig. 2 would be degenerate without SOC and would consist of one band with odd and another with even parity. Since the degeneracy is removed by SOC we can see two peaks, energetically close to each other.

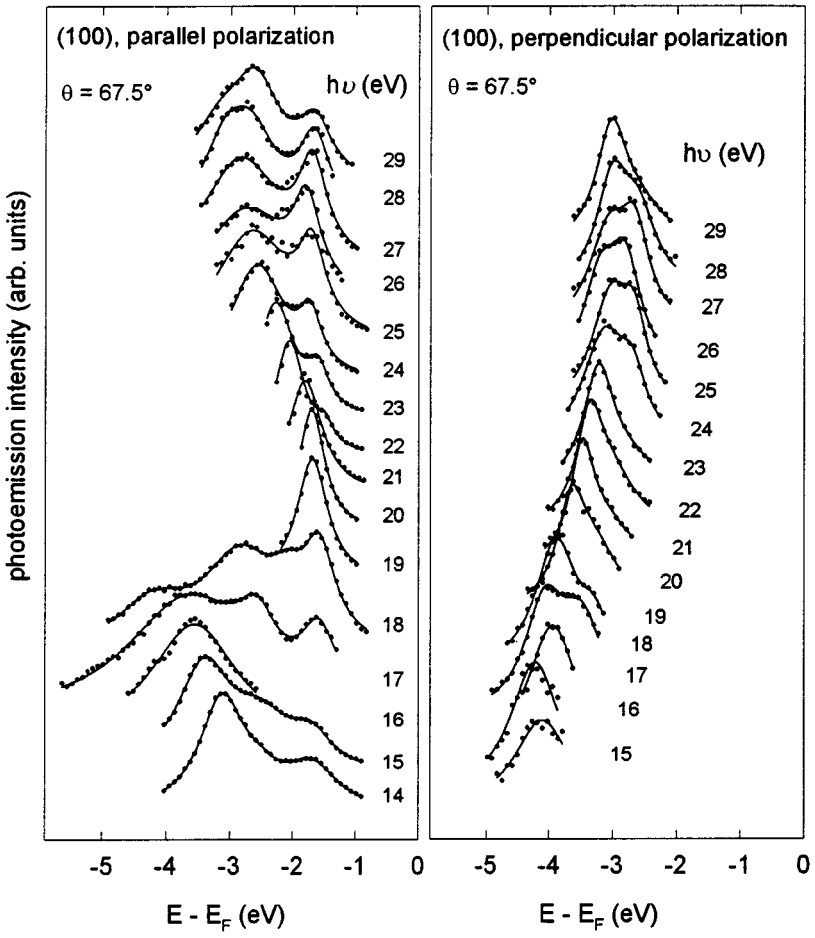

FIG. 6. ARPES spectra of PbS (dots) and their fit curves (lines), recorded for $\theta = 67.5°$ and $\hbar\omega$ between 14 and 29 eV. Both data and fit are shown in the fit region only, which was chosen in order to fit only the dominant features of the spectra. The ARPES shown in the left panel were recorded for parallel polarization with respect to the (100) observation plane, those of the right panel for perpendicular polarization.

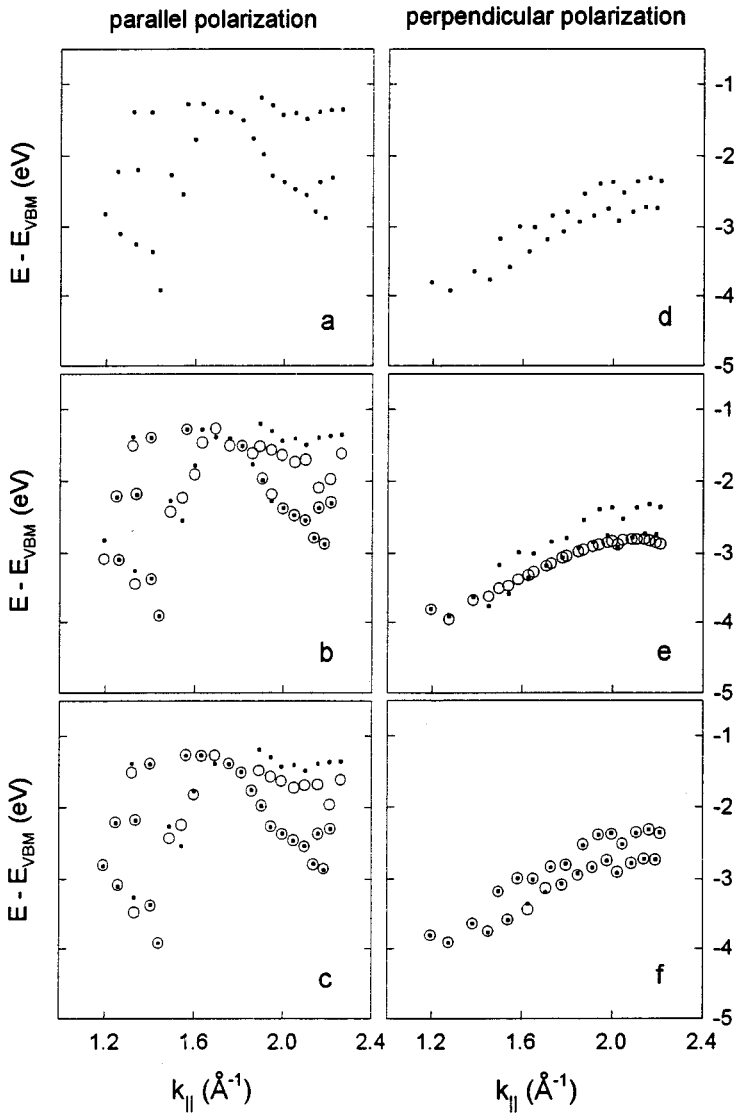

FIG. 7. Same as Fig. 4, here for the series with parallel and perpendicular polarization displayed in Fig. 6. For comparison of the calculated values without SOC [(b) and (e)] only bands with the "allowed" parity were used.

Nevertheless, remnants of the former band parity cause their different intensities. Usually, the peak derived from the band with former even parity appears merely as a shoulder of the other.

This is not true, however, for photon energies between 24 and 28 eV, corresponding to $k_{\parallel}$ between 1.9 and 2.2 Å^{-1}. We can shed some light on this phenomenon if we consider the fact that for $k_{\perp}^{\mathrm{red}} \approx 0$ states close to Γ ($k_{\parallel}=2.12$ Å^{-1}), the point with highest symmetry, are detected. In the vicinity of that point the third p-derived band meets the upper branch of the flat bands (see Fig. 2). Transitions from this band could therefore contribute to the intensity of the second peak in Fig. 6. Moreover, the presence of the third band is an additional perturbation of the wave functions, so that their initial symmetry may be further destroyed. The intensity increase vanishes completely when the path in k space leaves the neighborhood of the Γ point.

The resonance at $\hbar\omega=18$ eV may be caused by a similar scenario. Here, the parallel component of k is approximately 75% of the distance ΓX. At $k_{\perp}^{\mathrm{red}}=0$ this would coincide with the intersection of all three bands in the calculation without SOC. Although a quantitative comparison with the bands along Δ is improper for that photon energy (note that $k_{\perp}$ is not close to zero for $\hbar\omega<20$ eV), it is likely that again the interaction of all three p bands is responsible for the intensity gain of the weaker peak.

In the case of parallel polarization (left-hand panels in Figs. 6 and 7) up to four peaks contribute to the spectra and their energy positions are quite well reproduced by both calculations.

Using the complete calculation yields only minor improvements in this case. As in the spectra discussed so far, the most significant discrepancies between experiment and theory occur for the peak closest to the valence-band maximum, which is suspicious not to be characteristic for the bulk material.

VII. SUMMARY

Quite a few ARPES spectra recorded with synchrotron radiation in the (100) detection plane of PbS single crystals are analyzed and discussed. The measurements comprise normal emission data along the Δ line as well as off-normal emission for a variety of photon energies and emission

angles using different polarizations of the exciting radiation. The data agree very well with a pseudopotential band structure calculation including spin-orbit coupling. With the exception of a single structure at a binding energy of approximately -1 eV, all of the experimental peaks can be explained by assuming direct transitions between the calculated bulk bands. No need exists to invoke indirect transitions for the interpretation of the spectra. Moreover, the direct transition model turns out to be superior to the ODDS model, because the latter fails to account for the normal emission data. The consideration of SOC proves to be vital for the interpretation of ARPES in PbS. This is justified not only because a quantitative improvement can be achieved by the complete calculation, but also because a number of experimental peaks would be classified as forbidden when SOC is neglected. Nevertheless, different states contribute to the ARPES for parallel and perpendicular polarization of the light and the dominating structures of the spectra are predicted correctly by the Hermanson rule.

ACKNOWLEDGMENTS

We are very grateful to R. Baubinas for growing the excellent PbS crystals we used for our measurements. In addition we would like to thank the staff of BESSY for their professional work in general and for helping us out on many occasions in particular. Finally, we acknowledge the financial support by the Deutsche Forschungsgemeinschaft through the Sonderforschungsbereich 252 Darmstadt/Frankfurt/Mainz, and the Bundesminister für Forschung und Technologie under Contract No. 055RFAAI0.

[1] H. Y. Fan, Phys. Rev. **68**, 43 (1945); H. Thomas, Z. Phys. **147**, 395 (1957); H. Mayer and H. Thomas, *ibid.* **147**, 419 (1957); C. N. Berglund and W. E. Spicer, Phys. Rev. **136**, A1030 (1964).

[2] T. Grandke, L. Ley, and M. Cardona, Phys. Rev. Lett. **38**, 1033 (1977); Solid State Commun. **23**, 897 (1977); P. Heimann, H. Neddermeyer, and H. F. Roloff, Phys. Rev. Lett. **37**, 775 (1976).

[3] T. Grandke, L. Ley, and M. Cardona, Phys. Rev. B **18**, 3874 (1978).

[4] S. E. Kohn, P. Y. Yu, Y. Petroff, Y. R. Shen, Y. Tsang, and M. L. Cohen, Phys. Rev. B **8**, 1477 (1973).

[5] J. Hermanson, Solid State Commun. **22**, 9 (1977).

[6] See, for example, C. J. Bradley, and A. P. Cracknell, *The Mathematical Theory of Symmetry in Solids* (Clarendon, Oxford, 1972).

[7] V. Hinkel, H. Haak, C. Mariani, L. Sorba, K. Horn, and N. E. Christensen, Phys. Rev. B **40**, 5549 (1989).

[8] R. Böttner, N. Schroeder, E. Dietz, U. Gerhardt, W. Aβmus, and J. Kowalewski, Phys. Rev. B **41**, 8679 (1990).

[9] V. Kazlauskiene, J. Miskinis, J. Sinius, R. Baubinas, and J. Viatkus, J. Lithuanian Phys. **34**, 265 (1994) (in English by Allerton Press, USA).